Atmos. Chem. Phys., 4, 571–583, 2004
www.atmos-chem-phys.org/acp/4/571/
SRef-ID: 1680-7324/acp/2004-4-571

Atmospheric Chemistry and Physics

Validation of the calibration of a laser-induced fluorescence instrument for the measurement of OH radicals in the atmosphere

W. J. Bloss[1], J. D. Lee[1], C. Bloss[1], D. E. Heard[1], M. J. Pilling[1], K. Wirtz[2], M. Martin-Reviejo[2], and M. Siese[3]

[1]Department of Chemistry, University of Leeds, Woodhouse Lane, Leeds, LS2 9JT, UK
[2]Fundación CEAM, EUPHORE Laboratories, C/ Charles Darwin 14, Parque Technológico, 46980 Paterna, Valencia, Spain
[3]Institut für Chemie und Dynamik der Geosphäre, Institut II: Troposphäre, Forschungszentrum Jülich, D-52425 Jülich, Germany

Received: 28 October 2003 – Published in Atmos. Chem. Phys. Discuss.: 28 November 2003
Revised: 27 February 2004 – Accepted: 9 March 2004 – Published: 8 April 2004

Abstract. An assessment of the accuracy of OH concentrations measured in a smog chamber by a calibrated laser-induced fluorescence (LIF) instrument has been made, in the course of 9 experiments performed to study the photo-oxidation of benzene, toluene, 1,3,5-trimethylbenzene, para-xylene, ortho-cresol and ethene at the European Photoreactor facility (EUPHORE). The LIF system was calibrated via the water photolysis / ozone actinometry approach. OH concentrations were inferred from the instantaneous rate of removal of each hydrocarbon species (measured by FTIR or HPLC) via the appropriate rate coefficient for their reaction with OH, and compared with those obtained from the LIF system. Good agreement between the two approaches was found for all species with the exception of 1,3,5-trimethylbenzene, for which OH concentrations inferred from hydrocarbon removal were a factor of 3 lower than those measured by the LIF system. From the remaining 8 experiments, an overall value of 1.15±0.13 ($\pm 1\sigma$) was obtained for $[OH]_{LIF}$ / $[OH]_{HydrocarbonDecay}$, compared with the estimated uncertainty in the accuracy of the water photolysis / ozone actinometry OH calibration technique of 26% (1σ).

1 Introduction

Accurate measurements of trace gas concentrations are essential to study the chemistry of the Earth's atmosphere. Hydroxyl radicals (OH) are the principal oxidising species in the troposphere, and dominate the daytime removal of most volatile organic compounds (VOCs). Reaction with OH thus governs the atmospheric lifetime of many species, and hence their potential to contribute to (for example) global warming and ozone depletion. The OH-initiated oxidation of hydrocarbons and CO in the presence of oxides of nitrogen also leads to the generation of ozone, a constituent of photochemical smog. As the reactivity of OH is high, its concentration is low (of the order of 0.04–0.2 pptv in the sunlit troposphere) and chemical lifetime is short (0.1–1 s); OH concentrations are therefore determined by local chemical processes rather than transport, and their in situ measurement can be used to validate numerical models of tropospheric chemistry. Accurate measurement of atmospheric hydroxyl radical concentrations has been a goal of atmospheric scientists for three decades, following recognition of the central importance of OH radicals in tropospheric oxidation chemistry (Levy, 1971).

In-situ measurements of OH concentrations have been performed using radiometric, wet chemical and spin trapping techniques, however most recent measurements have been performed by the techniques of DOAS (Differential Optical Absorption Spectroscopy), LIF (Laser Induced Fluorescence) and CIMS (Chemical Ionisation Mass Spectrometry) (Heard and Pilling, 2003). CIMS and LIF are not absolute measurement techniques, and so require determination of the instrument response factor using an OH calibration source. The production of a well-known concentration of OH radicals at the instrument inlet under ambient atmospheric conditions presents a considerable challenge, and is critical to the accuracy of the current generation of LIF- and CIMS-based ambient OH measurement systems.

A series of photosmog experiments has recently been performed at the European Photoreactor Facility (EUPHORE), in Valencia, Spain, to study the oxidation of selected aromatic (and related) hydrocarbon species under polluted conditions. Instrumentation deployed included FTIR and HPLC for monitoring of hydrocarbon concentrations, and LIF for direct in situ measurement of OH concentrations. Under the conditions of the experiments, the dominant chemical removal route for the primary (initial) hydrocarbon species was by reaction with OH; thus OH concentrations could be calculated throughout each experiment, from the instantaneous

Correspondence to: W. J. Bloss
(w.bloss@chemistry.leeds.ac.uk)

rate of hydrocarbon decay via the relevant rate coefficient for reaction with OH, and compared with those obtained from the LIF instrument. In this way the accuracy of the LIF instrument measurements may be assessed.

The water photolysis/ozone actinometry approach used to calibrate the EUPHORE LIF system is commonly used in the calibration of field instruments for the measurement of ambient OH by LIF (Bloss et al., 2003; Holland et al., 2003; Kanaya et al., 2001). In this paper we present an assessment of the accuracy of this calibration based upon hydrocarbon decays measured in 9 photo-oxidation studies performed upon benzene, toluene, 1,3,5-trimethylbenzene, ethene, para-xylene and ortho-cresol.

2 The OH LIF system: description

The LIF system installed at the EUPHORE facility has been described in detail previously (Becker, 1999; Siese et al., 2001), therefore only a brief description of the instrument is given here. OH concentrations are measured by laser induced fluorescence at low pressure – the Fluorescence Assay by Gas Expansion (FAGE) technique (Hard et al., 1984): Ambient air is drawn through a small orifice into a fluorescence chamber, maintained at low pressure. A pulsed laser beam is directed through the gas expansion, leading to excitation of OH radicals through the (0,0) band of the ($A^2\Sigma^+ \leftarrow X^2\Pi_i$) transition near 308 nm. On-resonance (308 nm) fluorescence accompanying the subsequent relaxation of the OH ($A^2\Sigma^+$) is detected orthogonally to the gas expansion and excitation beam. Use of the low pressure chamber extends the OH fluorescence lifetime beyond the duration of the laser pulse, thus retrieval of scattered laser light can be minimised through temporal gating of the detection system. A high pulse-repetition-frequency (PRF), low pulse energy excitation beam is used to avoid optical saturation effects and minimise photolytic generation of OH from other chemical species. Excitation at 308 nm with on-resonance fluorescence monitoring is used rather than the alternative diagonal (1,0) fluorescence scheme with excitation near 282 nm in order to minimise generation of OH through the photolysis of ozone and subsequent reaction of $O(^1D)$ atoms with water vapour (Chan et al., 1990).

The EUPHORE LIF system uses a copper vapour laser pumped dye laser system (Oxford Lasers ACL 35/Lambda Physik FL3001) to generate 308 nm radiation at a PRF of 8.5 kHz. The laser power entering the fluorescence cell is typically 10–15 mW. A 0.38 mm diameter conically shaped nozzle is used to sample air from the EUPHORE chamber into the fluorescence cell, comprising a 100 mm aluminium cube maintained at a pressure of 1.6 mbar. Fluorescence is collimated through 75 mm optics and directed onto a microchannel plate photomultiplier tube detector through a 308 nm bandpass interference filter and an additional solar-blind filter. A concave mirror positioned opposite the detection axis approximately doubles the solid angle of fluorescence collected. Photon counting is used to monitor the amplified signal from the PMT, which is subsequently normalised by measured excitation laser power.

Contributions to the measured signal arise from OH LIF, and also from scattered laser and solar light, and detector dark current. Contributions from the latter sources are subtracted: Scattered laser light is measured by performing alternating measurements on- and off- the OH line; the latter containing no contribution from OH LIF. Scattered solar radiation is measured during a second photon counting window, several microseconds after each excitation laser pulse, at which time all OH LIF has decayed away - the contribution to the total signal from scattered sunlight is subtracted in this way, rather than through the off-line point, to avoid errors arising from changes in sunlight during the acquisition cycle. The on-line off-line cycle, yielding a single OH concentration measurement, typically takes 60–90 s, with variability between cycles being less than 5%.

3 The OH LIF system: calibration

LIF is not an absolute technique, thus calibration of the instrument response factor is required. The LIF signal per unit time (S) is proportional to the OH concentration and excitation laser power (P_{wr}), with the constant of proportionality or calibration constant C dependent upon factors such as the Einstein coefficients for the particular OH transition in question, rotational population, the overlap of the OH Doppler and laser spectral line widths and fluorescence collection efficiency:

$$S = C \times P_{wr} \times [\mathrm{OH}] \qquad (i)$$

While the value of C is in principle calculable (Stevens et al., 1994; Holland et al., 1995), in practice calibration with a known concentration of OH is required for accurate measurements. As noted above, during ambient measurements the total signal recorded contains contributions from scattered solar and laser light and detector dark current; S in Eq. (i) refers solely to the contribution from OH LIF.

The response of the EUPHORE LIF system was calibrated by the water photolysis – ozone actinometry method (Aschmutat et al., 1994). The calibration source consists of a 20 mm internal diameter by 600 mm length quartz tube, through which 20 slm (standard litres per minute) of humidified air was flowed, under approximately laminar conditions. The 184.9 nm radiation from a mercury pen-ray lamp was used to photolyse the water and oxygen within the tube, leading to the generation of OH, HO_2 and O_3 according to reactions (1)–(4), below:

$$H_2O + h\nu \rightarrow OH + H \qquad (1)$$

$$H + O_2 + M \rightarrow HO_2 + M \qquad (2)$$

$$O_2 + h\nu \rightarrow O + O \quad (3)$$

$$2 \times O + O_2 + M \rightarrow O_3 + M \quad (4)$$

After passing the photolysis region the calibration flow impinges upon the nozzle of the LIF system, and a fraction of the total flow (ca. 1 slm) is drawn into the instrument. The remainder of the flow is directed to an ozone monitor and subsequently vented. As the humidity of the air entering the flow reactor is known (measured using a chilled-mirror dew-point hygrometer) the concentration of OH or HO_2 radicals formed can be calculated from the measured ozone concentration and the relevant cross sections and quantum yields.

A complication arises due to the radial distribution of the axial flow velocity within the laminar flow tube: Air in the centre of the tube travels faster than air at the edges, and so spends less time in the photolysis region, and thus has lower OH, HO_2 and O_3 concentrations. The LIF nozzle samples from the centre of the flow tube, while the ozone concentration measured is the average of the remaining flow – a correction (the profile factor, P) must therefore be applied. For perfect laminar flow, with a parabolic velocity profile, and zero sample withdrawal by the LIF nozzle, the correction would be a factor of 2; for the EUPHORE calibration system a value of P=(1.85+/−0.09) has been measured (Siese et al., 2001).

The OH (or HO_2) concentration present at the LIF system sampling nozzle can then be calculated via Eq. (ii):

$$[OH] = \frac{[O_3] \times [H_2O] \times \sigma_{H_2O} \times \Phi_{OH}}{P \times [O_2] \times \sigma_{O_2} \times \Phi_{O_3}} \quad (ii)$$

where Φ_{OH} and Φ_{O_3}, the quantum yields for production of OH and (ultimately) O_3 from water and oxygen photolysis at 184.9 nm, have values of 1 (Sander et al., 2003) and 2 (Washida et al., 1971), respectively, P is the profile factor referred to above, and $\sigma(H_2O)$ and $\sigma(O_2)$ are absorption cross sections for water and oxygen (respectively) at 184.9 nm. A value of $(7.1\pm0.2)\times10^{-20}$ molecule^{-1} cm^2 is used for $\sigma(H_2O)$, being the mean of the determinations of Cantrell et al. (1997), Hofzumahaus et al. (1997) and Creasey et al. (2000). The emission spectrum of the 184.9 nm band from mercury pen-ray lamps overlaps with several features in the Schumann-Runge band of the O_2 spectrum (Lanzendorf et al., 1997). Under typical oxygen column densities employed for LIF calibration (ca. $(0.5–1)\times10^{19}$ molecule cm^{-2}), some absorption features within the lamp spectrum are saturated while others are not; thus the appropriate value of $\sigma(O_2)$ for calculation of O_2 photolysis in Eq. (ii) is dependent upon the actual oxygen column used. Moreover, the emission spectrum varies from lamp to lamp, and is dependent upon operating conditions (e.g. temperature, power) (Lanzendorf et al., 1997; Creasey et al., 2000). For the pen-ray lamp used in the EUPHORE LIF system, a value of $\sigma(O_2)=(1.23\pm0.05)\times10^{-20}$ molecule^{-1} cm^2 was determined under the actual operating conditions of oxygen column, lamp current and cooling flow employed in the calibration system.

Care is taken to work with sufficiently low photolysis flux that reactions between hydroxyl or hydroperoxy radicals and ozone (5–8, below) do not significantly alter their concentrations after generation and prior to sampling into the LIF cell:

$$OH + HO_2 \rightarrow H_2O + O_2 \quad (5)$$

$$OH + O_3 \rightarrow HO_2 + O_2 \quad (6)$$

$$OH + OH \rightarrow H_2O + O/H_2O_2 \quad (7)$$

$$HO_2 + O_3 \rightarrow OH + 2O_2 \quad (8)$$

Typical OH/HO_2 and O_3 concentrations generated were 7×10^8 molecule cm^{-3} and 7×10^{10} molecule cm^{-3}, respectively, with a flow tube residence time of less than 65 ms (between the photolysis region and sampling nozzle). Under these conditions, the fraction of OH lost through reactions (5), (6) and (7), and formed through reaction (8), is calculated to be equivalent to 0.5, 0.04, 0.02 and 0.001% (respectively) of the initial OH concentration.

The OH LIF signal is expected to decrease with increasing humidity in the sampled air, as H_2O is an extremely efficient quencher of electronically excited OH radicals: Relative values of k for the reaction

$$OH(A^2\Sigma^+, v'=0) + X \rightarrow OH(X^2\Pi_i, v'') + X \quad (9)$$

where X=N_2, O_2, H_2O are 1:4:20 at 294 K (Bailey et al., 1997, 1999), which equates to a calculated reduction in the total OH fluorescence quantum yield of approximately 7% from a totally dry atmosphere to one with 10 000 ppmv (1%) water vapour (typical of continental boundary layer air). However, the sensitivity of OH LIF systems has in some cases been observed to decrease with increasing humidity to a greater extent than can be explained by OH quenching alone (Holland et al., 1995; Hofzumahaus et al., 1996; Creasey et al., 1997a). The reduction in sensitivity (of up to 50% between 1000 ppmv (0.1%) and 10 000 ppmv (1%) H_2O) has been attributed to the formation of water clusters in the supersonic gas expansion, which scavenge OH and HO_2 (Holland et al., 1995): Temperatures in the supersonic expansion, which extends for a few tens of mm from the sampling nozzle into the fluorescence chamber, briefly dip to ca. 25 K; however the air rapidly warms – the OH rotational temperature at the point of LIF excitation is ca. 220 K (Creasey et al., 1997b). The humidity effect can be accounted for in the case of most tropospheric measurements by performing calibrations at ambient water vapour concentrations. In the EUPHORE chambers, absolute humidity is usually maintained at levels between 100 and 200 ppmv, much lower than ambient boundary layer values, in order to minimise interference in the FTIR spectra. Calibrations performed at this humidity are noisy (due to the low [OH] formed; Eq. ii), so routine

Table 1. Contributions to overall uncertainty in the OH calibration.

Contributing Factor	Fractional Uncertainty (1 s.d.)
H_2O 184.9 nm cross section	0.03
O_2 184.9 nm cross section	0.11 [a]
Flow profile P-factor	0.05
Humidity Dependence	0.15
Measurement of [H_2O]	0.02
Measurement of [O_3]	0.17
Overall Total	0.26

Notes a: Combined statistical uncertainty in the measurement of $\sigma(O_2)$ for the particular lamp used (4%), and estimated accuracy of the cross-section measurement procedure (10%) from Siese et al. (2001) and Creasey et al. (2000).

calibrations performed between photosmog experiments to check upon instrument performance were conducted at ca. 900 ppmv H_2O. In separate experiments the calibration constant was measured at water mixing ratios between 150 and 900 ppmv, and was found to be constant to within ±15%. Holland et al. (2003) report that nozzle design and diameter appear to be critical factors in determining the anomalous humidity dependence to the instrument calibration; using a shaped nozzle similar to that employed at EUPHORE (0.4 mm diameter) they observed a humidity dependence to the calibration constant consistent with the H_2O quenching mechanism alone.

The overall uncertainty in the calculated OH concentration (Eq. ii) and hence the instrument calibration arises from the various factors described above, and is summarised in Table 1. Addition of the various contributions in quadrature yields an overall uncertainty (1σ) in the calculated [OH] from the calibration source of 26%, with the dominant factor being the uncertainty in the measurement of ozone concentration, in particular noise in the zero measurement of the ozone instrument (Ansyco GmbH model 41 M) which at typical values of ±0.5 ppbv is significant compared to the measured ozone mixing ratios of 3–4 ppbv. Individual OH measurements will have a greater uncertainty, as their precision will be reduced by factors such as corrections for scattered solar and laser light, and the repeatability of excitation laser wavelength selection between on-line and off-line measurements – typically better than 5%.

4 Experimental

Measurements were performed in the course of the EXACT (Effects of the Atmospheric Oxidation of Aromatic Compounds in the Troposphere) programme at the European Photoreactor facility (EUPHORE) situated in Valencia, Spain during September 2001 and July 2002. The EXACT campaign and EUPHORE facility are detailed fully in Pilling (2003) and Becker (1997)/Klotz et al. (1998), respectively; only a brief overview and description of pertinent instrumentation is given here. The EXACT project aimed to elucidate the oxidation mechanisms for benzene, toluene, the xylenes and 1,3,5-trimethylbenzene, in the light of estimates that aromatic species could account for up to 30% of the total anthropogenic hydrocarbon oxidation initiated ozone production under European conditions (Derwent et al., 1996). The project combined laboratory studies and theoretical work to generate oxidation mechanisms for the target species within the Master Chemical Mechanism (MCM, http://www.chem.leeds.ac.uk/Atmospheric/MCM/mcmproj.html), with subsequent smog chamber experiments to test and refine the mechanisms. The data reported in this paper were acquired in the course of these validation experiments.

The EUPHORE chambers consist of two 195 m^3 volume hemi-spherical bags formed from FEP-teflon foil (with transmission greater than 80% between 280 and 640 nm) illuminated by natural sunlight. Hydraulically actuated steel housings exclude sunlight and protect the chambers from inclement weather when not in use. Chamber pressure is maintained at 100–200 Pa above ambient, and a floor cooling system is used to counteract solar heating during experiments. The chamber temperature is registered and approximately follows the ambient temperature (typically maintained at 25–35°C). The chambers are filled with ambient air, which is treated by an air purification and drying system to remove NO_y (<1 ppbv), H_2O (<200 ppmv) and non-methane hydrocarbons (<0.2 ppbv). Chamber mixing time is 2 min (fan assisted). Chamber A, used for all the experiments reported in this study, was equipped with the LIF system for OH radical measurement, a long-path FTIR interferometer system (Nicolet Magna 550, 326.8 m absorption path length; 1 cm^{-1} resolution) and off-line RP-HPLC system (HP 1050 series isocratic pump with diode array detector (HP 1100) and fluorescence detector HP1046A). Sampling of the polar ring retaining compounds for subsequent analysis by HPLC was performed using a double coil stripping system directly connected to the chamber. Additional instrumentation in chamber A included various ancillary monitors for O_3, NO_x, $J(NO_2)$ and meteorological parameters. For all the experiments discussed in this paper, hydrocarbon concentrations were monitored by FTIR; in the case of *o*-cresol measurements were made by HPLC also.

The conditions for each experiment are outlined in Table 2. Experiments were conducted by introducing the hydrocarbon species of interest together with the required concentration of NO/NO_2, allowing 10 min for mixing to occur, and then initiating the radical oxidation chemistry by opening the chamber covers to admit sunlight. During the experiments a certain amount of air from the chamber is lost through small leaks and withdrawal of air samples for analysis; clean air is added to compensate for this and some dilution of the reactants and

Table 2. Conditions for the photo-oxidation experiments and importance of chemical loss relative to dilution.

Run [a]	Hydrocarbon (HC) species	Initial HC vmr/ppb	Initial NO_x vmr/ppb	Chamber Temp./K [b]	$k_{Dilution}$ /10^{-5} s^{-1} [c]	Percentage Chemical Loss [d] Value	±1 s.d. Uncertainty
1	Toluene	512	509	302.3	1.61	74.6	7.7
2	1,3,5-TMB [e]	275	300	300.0	1.35	87.8	19.2
3	Toluene	500	150	302.3	1.58	66.0	11.9
4	Ethene	650	186	303.8	1.64	78.7	5.7
5	*o*-Cresol	300	40	299.2	1.37	92.9	2.9
6	*p*-Xylene	583	142	308.9	1.97	79.2	6.4
7	Benzene	1986	47	305.2	1.96	17.9	41.4
8	Benzene	1014	182	307.1	1.99	42.0	9.2
9	*p*-Xylene	248	155	304.9	1.97	85.0	2.6

Notes a: Chronological order in which experiments were performed, No.'s 1–5 during campaign 1, 6–9 during campaign 2.
b: Mean air temperature inside the chamber during the sunlit period.
c: Derived from SF_6 decay.
d: Fraction of the total hydrocarbon removal which arose from chemical reaction (balance from dilution).
e: Trimethylbenzene.

Table 3. Breakdown of chemical loss for each hydrocarbon species.

Run	Hydrocarbon species	Peak ozone/ppb [b]	Percentage of hydrocarbon loss by reaction with OH	O_3	NO_3	$O(^3P)$
1	Toluene	416	99.96	0.02	0.01	0
2	1,3,5-TMB	396	99.95	0.02	0.02	0.01
3	Toluene	255	99.97	0.02	0.02	0
4	Ethene	446	69.28	30.72	0	0
5	*o*-Cresol	107	12.04	0.05	87.91	0
6	*p*-Xylene	319	99.91	0.05	0.04	0
7	Benzene	177	99.92	0.05	0.03	0
8	Benzene	222	99.95	0.03	0.02	0
9	*p*-Xylene	362	99.92	0.05	0.03	0
Note a	Ethene	446	83.55	16.45	0	0
Note b	*o*-Cresol	107	98.30	0.04	1.67	0

Notes: Rate constants for ethene taken from Atkinson et al. (2002); for all other species from Calvert et al. (2002).
a: Correcting for the time-dependent growth in $[O_3]$ rather than using the peak value.
b: Correcting $[NO_3]$ for effect of reaction with cresol and other oxidation products via MCM simulation; see text.

products occurs as a result. To measure the dilution rate SF_6 was added to the reaction mixture as an inert tracer in each experiment and its concentration was monitored by FTIR. The average calculated loss rate of SF_6 over the course of each experiment (given in Table 2) was used as to calculate the contribution of dilution to the reduction in concentration of each hydrocarbon species.

In addition to dilution, removal of the primary hydrocarbon species (benzene, toluene, 1,3,5-trimethylbenzene, ethene, para-xylene and ortho-cresol) could in principle occur via photolysis, heterogeneous uptake and chemical reaction. Photolysis is unimportant for monocyclic aromatic hydrocarbons in the troposphere as their absorption spectra do not extend into the regions of the spectrum where significant actinic flux is encountered at low altitudes ($\sigma < 1\times10^{-19}$ molecule^{-1} cm^2 at 285 nm) and decreasing to higher wavelengths for all aromatic species considered here (Calvert et al., 2002; Etzkorn et al., 1999). Similar comments apply to the photochemistry of ethene (Atkinson, 1990). The particulate loading of the purified air used to fill the EUPHORE chambers is low (<50 particles cm^{-3}) and aerosol yields from the monocyclic aromatic species considered are low under the conditions of the EXACT experiments (Pilling, 2003) thus heterogeneous losses are not expected to be a significant sink for the primary hydrocarbon species considered here; rather chemical reaction dominates their active removal.

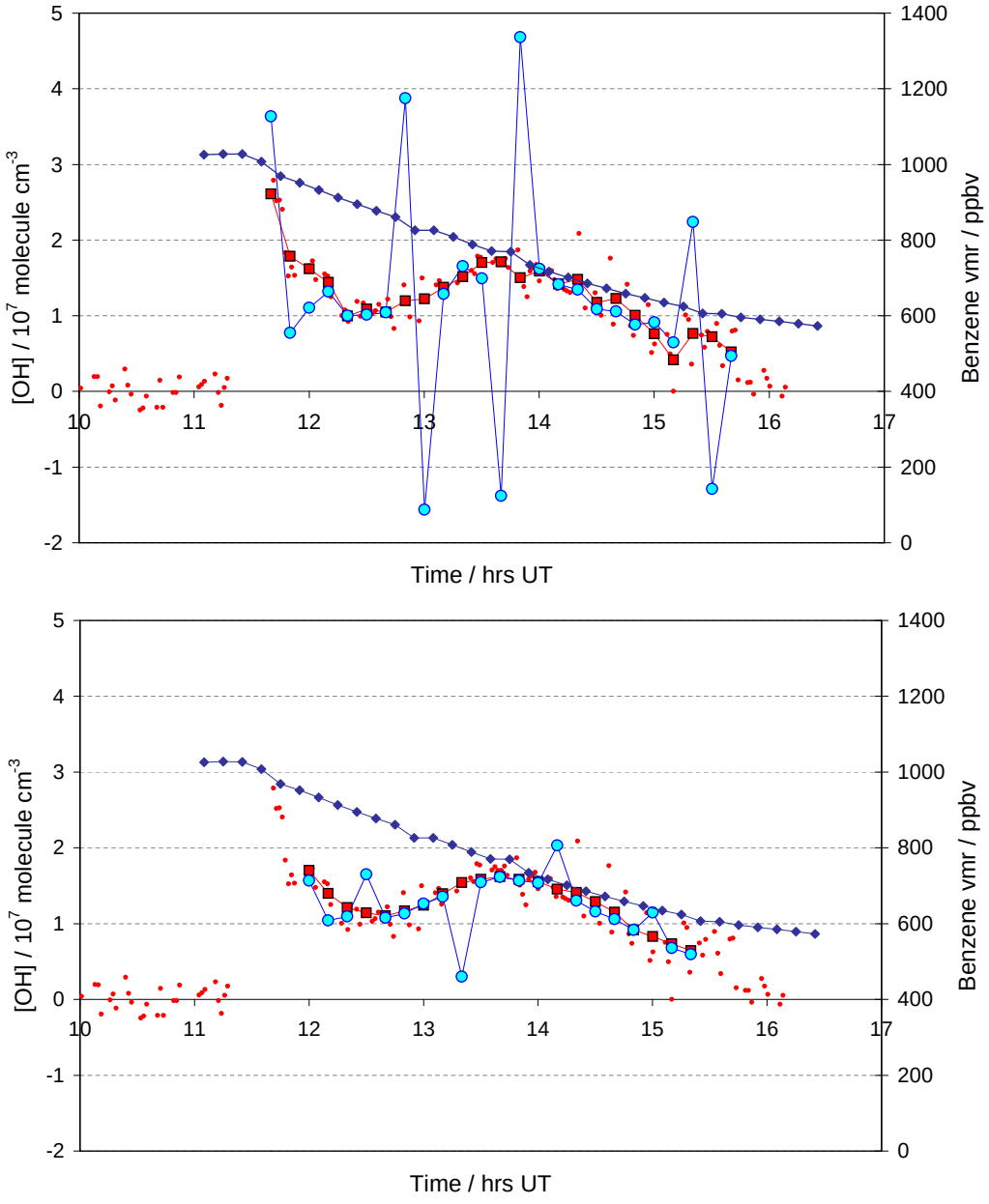

Fig. 1. Effect of lengthening the analysis period from successive hydrocarbon measurement points (1-point, top panel) to every fifth hydrocarbon measurement point (5-point, lower panel). Scatter and noise are greatly reduced in the latter instance. Data for benzene, experiment (8). Key: Benzene mixing ratio, blue diamonds; individual [OH] from LIF, small red circles; [OH] inferred from benzene decay; blue circles; average LIF [OH] over the corresponding interval between benzene measurements, black/red squares.

In the lower atmosphere, reaction with O_3, OH, NO_3 and $O(^3P)$ have been identified as the key processes which initiate the oxidation of aromatic hydrocarbons (Atkinson, 1994). Table 3 lists the percentage contribution to the removal of each hydrocarbon species for reaction with O_3, OH, NO_3 and $O(^3P)$, under the conditions of the experiments performed. Values were calculated to give a "worst case" value from the perspective of the importance of reaction with OH: While mean OH concentrations (as measured by LIF) were used, concentrations of O_3, NO_3 and $O(^3P)$ were all upper limits: The peak ozone concentration for each experiment is used, while in practice the mean ozone concentration is much lower. NO_3 concentrations were calculated from simple photochemical steady state (formation via NO_2+O_3; loss via photolysis), while in practice NO_3 concentrations will be lowered by reaction with NO, NO_2, hydrocarbons etc. $O(^3P)$ concentrations were calculated from measured [O_3] and calculated $J(O_3)$, assuming that all $O(^1D)$ was quenched to $O(^3P)$ and that all $O(^3P)$ only underwent reaction with O_2.

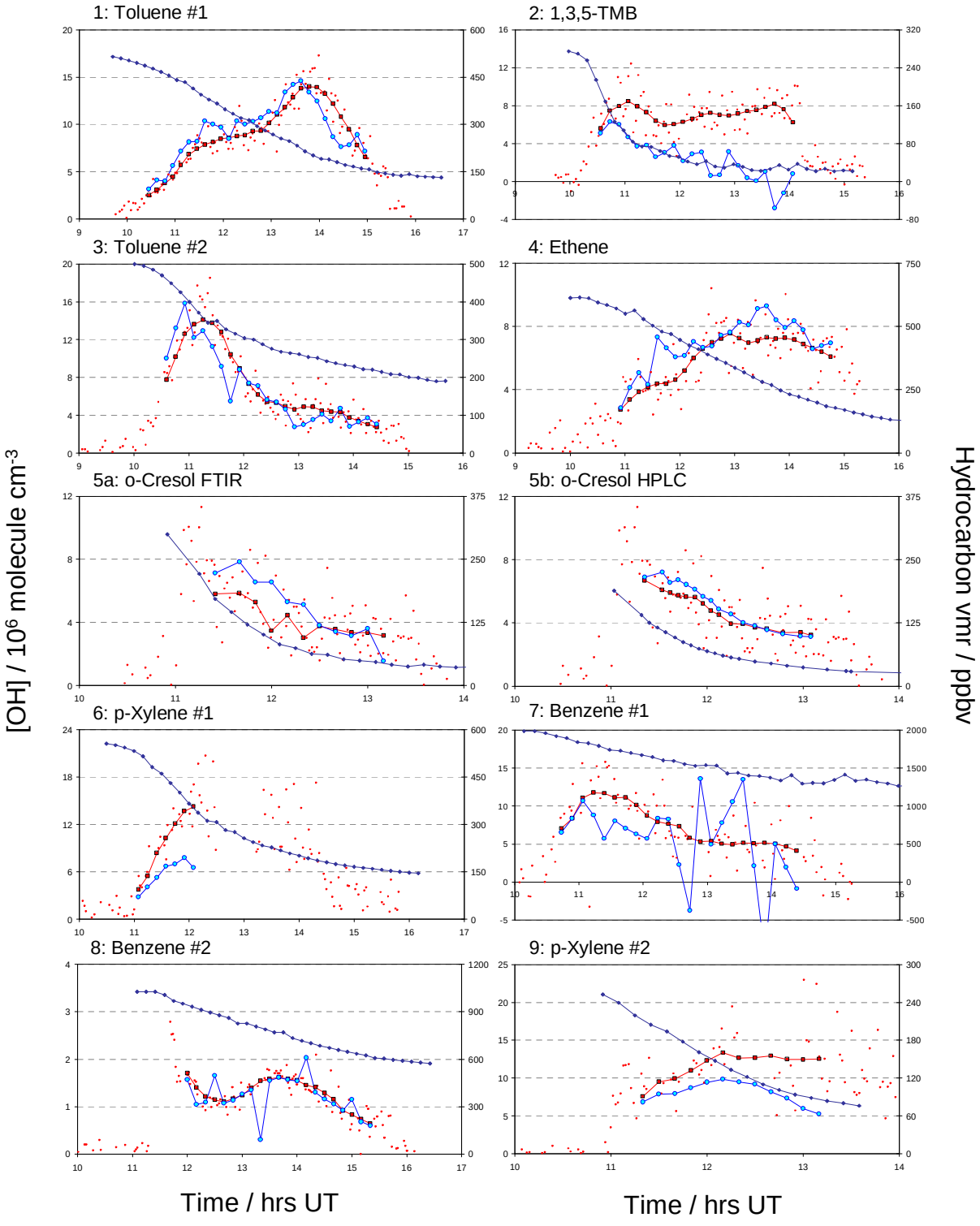

Fig. 2. Data from each experiment showing comparison between measured and inferred OH concentrations. Key: Individual [OH] from the LIF measurements, small red circles; [OH] from LIF averaged over interval between hydrocarbon measurements used for analysis, black/red squares; [OH] inferred from hydrocarbon decay, blue circles; hydrocarbon mixing ratio, blue diamonds (right hand abscissa; vmr=volume mixing ratio).

It can be seen from Table 3 that reaction with OH accounts for more than 99.9% of the loss of each hydrocarbon species, with the exceptions of ethene and *o*-cresol, for which reaction with O_3 and NO_3 (respectively) is significant. In the case of the ethene experiment (4), ozone mixing ratios increased from <1 ppbv to 446 ppb over the course of 5 h, thus the mean removal of ethene by ozone was rather lower than line 4 of Table 3 suggests, at 16.4%. The contribution of ozonolysis to the removal of ethene was accounted for as detailed in Sect. 5, below.

Considering the case of *o*-cresol, the NO_3 concentration obtained from the simple steady-state approach (in which photolysis is the only sink for NO_3), ca. 1.8×10^8 molecule cm^{-3}, is greatly overestimated as NO_3 will react with many species present, not least *o*-cresol itself. Inclusion of this reaction alone as an additional NO_3 sink in the steady state analysis reduces the calculated mean [NO_3] to 7.3×10^5 molecule cm^{-3}, and reduces the significance of NO_3 for removal of cresol to 5%. This is also an overestimate, as the primary fate of NO_3 was reaction with products of cresol oxidation – a simulation of the cresol oxidation system, performed using the MCM version 3.1 (Pilling, 2003) employing all relevant reactions and initiated with measured concentrations, determined that 28% of the loss of NO_3 was by reaction with cresol, less than 0.1% by photolysis and the remainder by reaction with products of cresol oxidation. The same simulation determined that, after dilution, over 98% of the removal of cresol occurred through reaction with OH.

The removal of the primary hydrocarbon species is thus overwhelmingly dominated by reaction with OH (after accounting for dilution, and the ozonolysis reaction in the case of ethene), and the hydrocarbon decay data can be used to infer the concentration of OH radicals present.

5 Inferred OH from hydrocarbon decays: method

For each experiment, a subset of hydrocarbon and OH data was selected corresponding to the period during which the chamber was open to sunlight (typically 3–5 h). The hydrocarbon concentration-time data were analysed using the interval method (Guggenheim, 1926) to obtain a pseudo-first-order rate coefficient (k') for hydrocarbon removal:

$$k' = \ln(c_1/c_2)/(t_2 - t_1) \qquad (iii)$$

where c_1 and c_2 were the hydrocarbon concentrations measured at times t_1 and t_2, respectively. The mean OH concentration during the time period between t_1 and t_2 was then obtained via

$$[OH]_{HC}=(k'-k_{dil})/k_{OH+HC} \qquad (iv)$$

where k_{dil} is a first-order rate coefficient for the effect of dilution and k_{OH+HC} is the rate coefficient for the reaction between OH radicals and the hydrocarbon species in question, at the appropriate temperature (Table 2) and atmospheric pressure.

The treatment of the ethene data (experiment 4) was an exception to the above procedure: In this system, reaction with ozone accounts for between 1 and 30% of the chemical loss of ethene, depending upon the time-point considered. Equation (iv) were therefore modified to include a term accounting for the ozonolysis reaction, and the ethene data were analysed to return $[OH]_{HC}$ according to Eq. (v):

$$[OH]_{HC}=(k'-k_{dil}-k_{C2H4+O3}[O_3])/k_{OH+HC} \qquad (v)$$

A value of 1.87×10^{-18} molecule^{-1} cm^3 s^{-1} was used for $k_{C_2H_4+O_3}$ (Atkinson et al., 2002). Analysis of the ethene data was otherwise identical to that for the other hydrocarbon species, as described below.

Each inferred OH concentration was compared with the mean value for [OH] obtained by the LIF instrument, $[OH]_{LIF}$, over the same time period (t_1 to t_2). The overall agreement for each species/experiment was quantified by calculating the ratio, R, of the sum of the values of [OH] obtained from the averaged LIF measurements to the equivalent from the hydrocarbon decay data:

$$R=\Sigma[OH]_{LIF}/\Sigma[OH]_{HC} \qquad (vi)$$

Thus a value of unity for R indicates perfect agreement, values greater than 1 indicate that OH concentrations measured by the LIF system were greater than those inferred from the hydrocarbon decay and suggest that the calibration constant C (Eq. i) may be too small, and values less than 1 suggest the converse.

Random noise in the hydrocarbon concentrations obtained from the FTIR data leads to a high degree of variability in the inferred OH concentrations, as can be seen in Fig. 1a, showing the results for benzene (experiment 8); in some cases negative OH concentrations are returned. This variability can be reduced by increasing the time interval between each pair of hydrocarbon concentrations analysed. In this work a 5-hydrocarbon measurement point interval (ca. 40 min) gave a reasonable balance between reducing the noise in the inferred OH concentrations and maintaining a significant number of data points in the analysis; thus the first inferred OH concentration was obtained from hydrocarbon concentrations c_1 and c_5, the second from c_2 and c_6, and so forth. The OH concentrations obtained from the LIF system were averaged over the same time interval, i.e. t_1 to t_5, t_2 to t_6 etc. corresponding typically to 15–20 individual OH measurements (each taken at 90–120 s intervals) for each value of $[OH]_{LIF}$. Figure 1b shows the reduced variability in inferred OH concentration with a 5-point interval between benzene concentrations. The value of R obtained is equal (to within 1%) in each case; however the reduction in scatter accompanying adoption of the 5-point interval greatly facilitates visual comparison of the values of $[OH]_{HC}$ and $[OH]_{LIF}$.

Rate coefficients for the reaction of OH with the various hydrocarbon species, k_{OH+HC}, as given in Table 4, were

Table 4. Literature values for k(OH+HC) and ratio of LIF-measured to hydrocarbon-inferred OH concentrations.

Run	Hydrocarbon species	k(OH+hydrocarbon) /10^{-12} molecule^{-1} cm^3 s^{-1} [a]	R=Σ[OH]$_{LIF}$/Σ[OH]$_{HC}$ Value [b]	+/− Uncertainty [c]
1	Toluene	5.51	0.96	0.19
2	1,3,5-TMB	56.7	3.02	0.60
3	Toluene	5.51	1.06	0.21
4	Ethene	8.04 [d]	0.87	0.21
5a	*o*-Cresol (FTIR)	40.7	0.83	0.25
5b	*o*-Cresol (HPLC)	40.7	0.93	0.28
6	*p*-Xylene	14.3	1.69	0.42
7	Benzene	1.24	1.29	0.26
8	Benzene	1.24	1.04	0.21
9	*p*-Xylene	14.3	1.45	0.36

Notes a: Recommended values from Calvert et al. (2002).
b: R defined as in Eq. (vi).
c: Uncertainty quoted here derived from uncertainty in k(OH+Hydrocarbon) only.
d: Mean of values from Atkinson et al. (2002) and Sander et al. (2003).

taken from Calvert et al. (2002), with the exception of ethene, for which the mean of the values recommended by the IUPAC (Atkinson et al., 2002) and NASA/JPL (Sander et al., 2003) panels was used. Uncertainty in the individual values is discussed further below.

6 Inferred OH from hydrocarbon decays: results

The hydrocarbon decay data, individual measured LIF OH concentrations, inferred OH concentrations $[OH]_{HC}$ and averaged LIF OH concentrations $[OH]_{LIF}$ are shown in Fig. 2. Table 4 lists the value of the OH+ hydrocarbon rate coefficient used to evaluate each dataset, and gives the values of R, the ratio of $[OH]_{LIF}$ to $[OH]_{HC}$, obtained. The uncertainty quoted in Table 4 reflects the uncertainty in the rate coefficient, k_{OH+HC} only – the value of R is directly proportional to k_{OH+HC} via Eqs. (iv) and (vi). Figure 3 compares the values of R obtained for each experiment, with two confidence intervals shown – the inner limits reflecting solely uncertainty in k_{OH+HC}, as given in Table 4, and the outer limits reflecting the propagation of this with the uncertainty (26%) in the LIF system calibration. The results for each individual species are discussed below.

6.1 Toluene

Experiments (1) and (3) show excellent agreement between the LIF and hydrocarbon-inferred (HC) values for OH, with values for R of (0.96±0.19) and (1.06±0.21) obtained, respectively.

6.2 1,3,5-Trimethylbenzene

The OH concentrations obtained from the LIF and HC analyses are not in agreement for 1,3,5-TMB (trimethylbenzene), with the LIF data considerably higher than the hydrocarbon decay giving R=(3.0±0.6). The quality of the hydrocarbon decay data is poor (reflecting the lower 1,3,5-TMB concentrations used in this experiment) which contributes to the variability in the $[OH]_{HC}$ values, but cannot explain the discrepancy between the absolute values, possible reasons for which are discussed in Sect. 7.

6.3 Ethene

The OH concentrations inferred from the decay of ethene are in good agreement with those measured by the LIF system throughout the experiment, giving a value of R=(0.87±0.21). The correlation in the shape of the OH profiles indicates that the modified analysis to account for the ozonolysis reaction (Eq. v) is correct, as the contribution to chemical loss of ethene from this reaction ranges from 1.5% for the first point to 39.6% for the final point.

6.4 *o*-Cresol

The cresol experiments show good agreement between OH concentrations measured directly by LIF and inferred from the hydrocarbon decays, with values of R=(0.83±0.25) and (0.93±0.28) for the FTIR and HPLC analyses, respectively. The HPLC data are smoother than those from the FTIR, reflected in reduced noise in the values of $[OH]_{HC}$ in Fig. 2f. Differences in the $[OH]_{LIF}$ data between Figs. 2e and 2f reflect the FTIR and HPLC data being acquired on different timescales, and thus different averaging of the individual LIF data points being applied.

6.5 para-Xylene

The data from the first *p*-xylene experiment (6) is limited due to a partial power failure, which interrupted OH data

acquisition at approximately 12:30 pm. While data acquisition resumed 90 min later, confidence in the validity of the OH calibration was low as the dye laser beam alignment had to be completely reoptimised, and no check of the instrument calibration was possible until the next day; therefore only data acquired prior to the power failure are considered. Agreement between $[OH]_{HC}$ and $[OH]_{LIF}$ is poor for experiment (6), R=(1.69±0.42), better for experiment (9), R=(1.45±0.36) considering just the uncertainty in the OH+p-xylene rate coefficient, and R=(1.45±0.52) if the uncertainty in the LIF calibration is factored in (as shown in Fig. 3). Again, possible reasons for the disagreement are considered below.

6.6 Benzene

The contribution of chemical loss (reaction with OH) to the total loss of benzene is the least of all the species considered (Table 2); dilution dominates due to the low rate coefficient for the benzene +OH reaction. Accordingly the values of $[OH]_{HC}$ obtained are noisier, as scatter in the FTIR retrievals has a greater influence. The absolute agreement between the LIF and HC [OH] is good for experiment (7) (Fig. 2i) and excellent for experiment (8) (Fig. 1), with values of R=(1.29±0.26) and (1.04±0.21) obtained, although inspection of the plot indicates that the confidence interval, reflecting uncertainty in k(OH+benzene), is probably underestimated for experiment (7).

7 Conclusions

The principal factor affecting the value of R, the measure of absolute agreement between HC and LIF values for [OH], is the rate coefficient used for the hydrocarbon – hydroxyl reaction (Eq. iv). Studies of the relevant rate coefficients have been reviewed by Calvert et al. (2002), recommended values from which are used in this work; however the discrepancies observed in the cases of 135-TMB and p-xylene merit further attention.

Measurements of k(OH+1,3,5-TMB) at 298 K range from $(3.78\pm0.52)\times10^{-11}$ molecule^{-1} cm^3 s^{-1} (Ohta and Ohyama, 1985) to $(6.24\pm0.75)\times10^{-11}$ molecule^{-1} cm^3 s^{-1} (Perry et al., 1977), with a recommended value (Calvert et al., 2002) of k(OH+1,3,5-TMB)=$(5.67\pm1.13)\times10^{-11}$ molecule^{-1} cm^3 s^{-1}. Adoption of the lowest measured value (3.78×10^{-11} molecule^{-1} cm^3 s^{-1}) would reduce the value of R obtained from this experiment by 33%, to (2.01±0.59) (confidence interval reflects combined uncertainty in k and the LIF calibration). Uncertainty in the kinetic data can thus account for some, but not all, of the discrepancy between $[OH]_{HC}$ and $[OH]_{LIF}$ in the 1,3,5-TMB experiment. For p-xylene, measurements of k(OH+p-xylene) exhibit significant scatter, ranging from $(1.05\pm0.1)\times10^{-11}$ molecule^{-1} cm^3 s^{-1} (Ravishankara et al., 1978) to $(1.82\pm 0.22)\times10^{-11}$ molecule^{-1} cm^3 s^{-1} (Perry et al., 1977) with the recommendation of Calvert et al. (2002), of $(1.43\pm0.36)\times10^{-11}$ molecule^{-1} cm^3 s^{-1} being a straight average of a subset of the recent determinations. Were the lower measurement of 1.05×10^{-11} molecule^{-1} cm^3 s^{-1} to be adopted, the values of R for the p-xylene experiments would be reduced by 27% to (1.24 ±0.35) and (1.06±0.30) for experiments (6) and (9), respectively, in good agreement with the values from the other species considered (again, confidence interval reflects combined uncertainty in k and the LIF calibration). The results of this work therefore suggest that the true value for k(OH+p-xylene) may be somewhat lower than the value recommended by Calvert et al. (2002).

If the values for the rate constants (k_{OH+HC}) used are correct, the sense of discrepancy which might be anticipated in this work (assuming all other factors to be correct) is $[OH]_{HC} > [OH]_{LIF}$ – which could arise if processes other than dilution and reaction with OH contributed to the removal of the hydrocarbon species. Disagreement in the opposite sense (as observed for 1,3,5-TMB and p-xylene) implies either regeneration of the primary hydrocarbon (for which no mechanism can be envisaged) or a problem with the values of $[OH]_{HC}$ or $[OH]_{LIF}$. Other sources of loss of the hydrocarbon species have been discussed (Sect. 4); however two potential systematic errors in the values of $[OH]_{HC}$ and $[OH]_{LIF}$ are considered below: Errors in the FTIR retrievals of the hydrocarbon concentrations, and generation of artefact OH radicals, through photolysis of sampled compounds by the excitation laser pulse.

The pseudo-first order nature of the analysis leads to the inferred OH concentrations, $[OH]_{HC}$, being independent of the absolute hydrocarbon concentrations, and hence of the cross sections used to analyse the FTIR data, and standards adopted to calibrate the HPLC instrument. Errors in the retrieved hydrocarbon concentrations, for example due to overlap with absorption spectra of photo-oxidation products, could however lead to incorrect values for $[OH]_{HC}$. Such spectral contamination would be expected to vary (and worsen) over the course of the experiments, as the complexity of the analyte increased and the primary hydrocarbon concentration decreased, and thus any deviation between $[OH]_{HC}$ and $[OH]_{LIF}$ would be expected to increase. This trend is observed in the case of 1,3,5-TMB (experiment 2), and to a lesser extent in the case of p-xylene. In the case of 1,3,5-TMB however no spectral overlap occurs between the trimethybenzene and the two major photo-oxidation products, methylglyoxal and PAN. The 1,3,5-TMB concentrations obtained from the FTIR analysis are in good agreement (better than 1%) with those obtained from GC-FID measurements performed during the same experiment, at the start of the 1,3,5-TMB decay; however when the 1,3,5-TMB mixing ratio falls below ca. 75 ppbv (25% of the initial level), the FTIR concentrations begin to exceed those from the GC-FID. The discrepancy reaches approximately 15 ppbv (equivalent to 50%) by the end of the experiment, suggesting that the

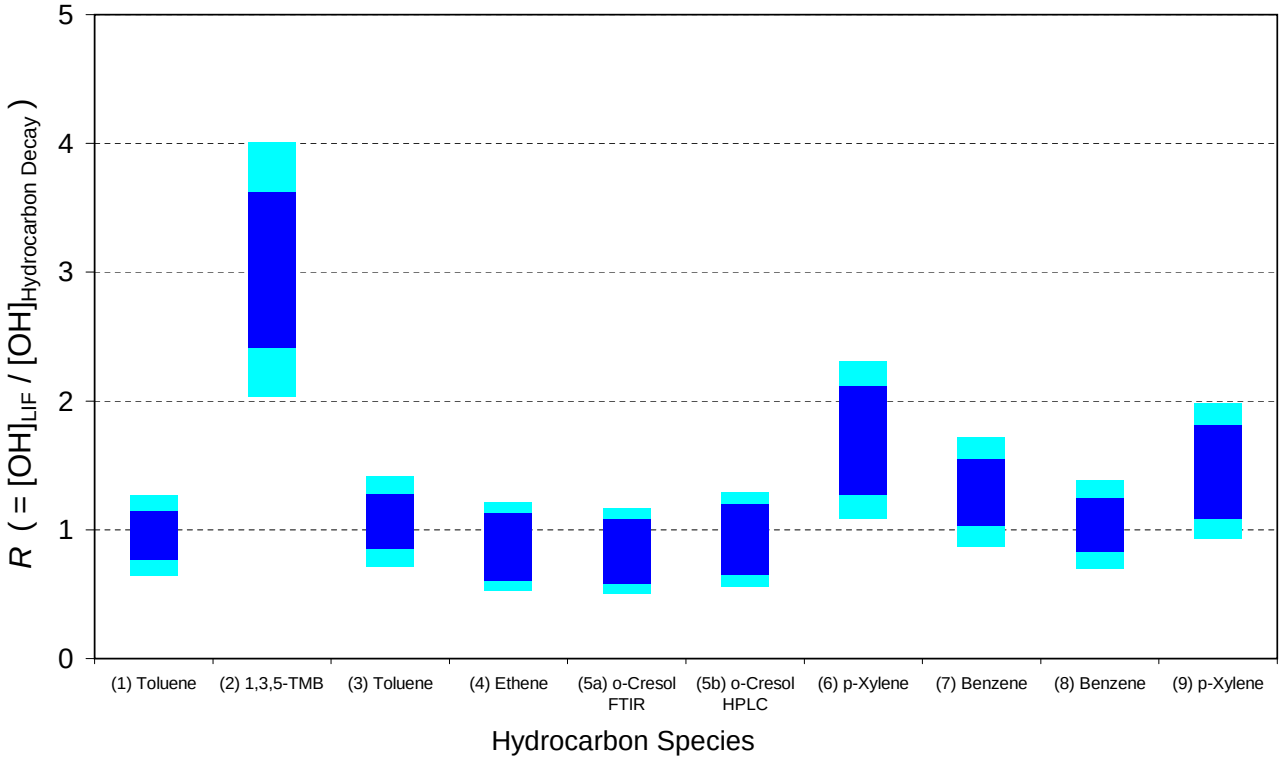

Fig. 3. Ratio (R) of OH concentrations measured by the LIF system and those obtained from hydrocarbon decay data. Outer (light blue) confidence interval indicates combined uncertainty in FAGE calibration (26%) and k(OH+Hydrocarbon) (Table 4); inner confidence interval reflects uncertainty in k(OH+Hydrocarbon) only.

FTIR data may indeed be suffering from spectral contamination, as considered above, in this experiment. The statistical uncertainty in the FTIR and HPLC data is low – estimated to be 2% and 4%, respectively – and is not included in the uncertainties calculated for R (Table 4), as while this factor will contribute to point-to-point scatter in the inferred $[OH]_{HC}$, it will not impart a systematic error to the value of R.

The photolysis of ambient ozone, generating $O(^1D)$ which could react with ambient water vapour to form OH radicals, was a problem for some early measurements of OH by LIF, in which 282 nm excitation was used (Zeng et al., 1998). Use of 308 nm excitation, combined with high PRF – low pulse energy excitation, reduces the contribution to returned [OH] from this source to less than 10^3 molecule cm^{-3} under conditions of the EUPHORE experiments ($[O_3]$, $[H_2O]$, laser fluence). Hydrocarbon photolysis by the excitation laser beam could also lead to artefact OH generation; however no significant levels of OH were detected ($<1\times10^6$ molecule cm^{-3}) at the start of each experiment, when the hydrocarbon species had been introduced to the chamber but prior to opening of the covers to admit sunlight (Fig. 2). Photolysis of products of the oxidation of each primary hydrocarbon could contribute to artefact OH generation; however considering the case of 1,3,5-TMB, the three principal observed products were methyl glyoxal, PAN and HCHO. If direct production of OH radicals with unit quantum yield following 308 nm photolysis of each of these species were possible, the maximum concentrations of OH radicals produced inside the FAGE cell would be ca. 2500, 75 and 1500 molecule cm^{-3}, respectively (calculated for the maximum concentration of each species observed, using the measured LIF cell pressure (1.6 mbar) and typical observed OH rotational temperature (220 K)). These values can be compared to a concentration of ca. 17 000 molecule cm^{-3} of OH within the FAGE cell which results from sampling ambient air containing $[OH]=8\times10^6$ molecule cm^{-3} (typical of the levels found during the 1,3,5-TMB experiment). When the further requirements for any such OH to be generated in the correct rovibronic state, and to be both generated and excited within the same laser pulse are considered, the contribution of photolytic artefacts to the returned [OH] is clearly minimal.

Variation in the calibration of the LIF system between experiments could account for the discrepancies in the results for 1,3,5-TMB – calibration of the LIF system requires entry into the EUPHORE chamber, which must be purged of experimental gases prior to calibration, and of water vapour etc. afterwards. Therefore, it was not possible to perform calibration checks between every experiment during the EXACT campaigns. Calibrations performed at the start and end of the first exact campaign were within 6% of each other; similarly for the second campaign, 17 individual calibrations performed on three different days at the start, middle and end

of the campaign exhibited a standard deviation of 9%. It is therefore unlikely that variation in the instrument calibration (arising for example from variations in laser linewidth due to changed oscillator alignment) can explain the large discrepancies obtained for 1,3,5-TMB and *p*-xylene. This conclusion is supported by the excellent agreement between the two toluene experiments, (1) and (3), performed prior and subsequent to the 1,3,5-TMB run, and by the consistency in the result from the two *p*-xylene runs, which were conducted 15 days apart.

No single reason can be identified for the disagreement between values of $[OH]_{LIF}$ and $[OH]_{HC}$ in the case of 1,3,5-TMB; uncertainty in the rate constant for reaction with OH can account for some, but not all of the discrepancy. Comparison of the GC-FID concentration measurements obtained for 1,3,5-TMB during experiment (2) with those from the FTIR system suggest that instrumental rather than chemical causes may be responsible for the discrepancy. In the case of *p*-xylene, agreement (within 1 s.d. uncertainty) is achieved for experiment (9), and nearly for experiment (6) (Fig. 3); as discussed above, k(OH+*p*-xylene) may be somewhat smaller than that used to obtain these values. The confidence interval in the values of R listed in Table 4 reflect only the uncertainty in k(OH+hydrocarbon), and those plotted in Fig. 3 show also the combined uncertainty in the calculated [OH] from calibration. The true uncertainty in these values is larger, as no contribution from data scatter is included – for example, inspection of Fig. 2 indicates clearly that the value of R obtained from experiment (7) will be less precise than that from experiment (1).

We discount the results from experiment (2) (1,3,5-TMB) from our final comparison between the LIF-measured and hydrocarbon-inferred OH, on the basis that the deviation in this case is much greater than indicated by the remaining studies, and is likely to be due to some other systematic factor. Averaging results from the remaining 8 experiments gives a mean value for $[OH]_{LIF}/[OH]_{HC}$ of (1.15±0.13), where the range indicates combined (1 s.d.) uncertainty in the values of k(OH+hydrocarbon) and the LIF calibration methodology. This result thus indicates that OH concentrations retrieved from LIF systems calibrated using the water-photolysis ozone-actinometry calibration approach are accurate to within the stated calibration uncertainty (±26%), but suggests a slight bias to overestimate the true ambient OH concentration. The possibility of counterbalancing errors in the various calibration factors (e.g. oxygen and water cross sections) is not precluded, so the same conclusion cannot necessarily be drawn for the analogous calibration approach in which photolysis of water vapour is quantified through measurement of the UV flux by a calibrated photodiode.

The results of this work indicate that OH concentrations measured by an LIF instrument calibrated using the water photolysis-ozone actinometry method are accurate to within the stated calibration uncertainty of ±26%, with a mean value of $[OH]_{LIF}/[OH]_{\text{hydrocarbon decay}}$ of (1.15±0.13) obtained. Continuing development of calibration techniques, for example via the ozonolysis of alkenes (Hard et al., 2002), and further intercomparisons of ambient OH measurements performed using different approaches and calibration techniques, such as the comparison between LIF and DOAS techniques reported by Brauers et al. (1996), are essential to further our understanding of the accuracy and precision of the current generation of hydroxyl radical measurements.

Acknowledgements. Fundación CEAM is supported by Generalidad Valenciana and BANCAIXA. Financial support for this work was provided through the EU programme "Effects of the Oxidation of Aromatic Compounds in the Troposphere" (EXACT), Contract #EVK2-CT-1999-00053, and Ministerio de Ciencia y Tecnología (REN2000-3277-CE/CLI, REN2001-4600-E /CLI).

Edited by: A. Volz-Thomas

References

Aschmutat, U., Hessling, M., Holland, F., and Hofzumahaus, A.: A tunable source of hydroxyl (OH) and hydroperoxy (HO_2) radicals: In the range between 10^6 and 10^9 cm^{-3}, Physico-Chemical Behaviour of Atmospheric Pollutants, edited by Angeletti, G. and Restelli, C., Proc. EUR 15609, 811–816, 1994.

Atkinson, R.: Gas-phase Tropospheric Chemistry of Organic Compounds: A review, Atmos. Environ. 24A, 1, 1–41, 1990.

Atkinson, R.: Gas Phase Tropospheric Chemistry of Organic Compounds, J. Phys. Chem. Ref. Data, Monograph No. 2, 1–216, 1994.

Atkinson, R., Baulch, D. L., Cox, R. A., Crowley, J. N., Hampson, R. F., Kerr, J. A., Rossi, M. J., and Troe, J.: Summary of Evaluated Kinetic and Photochemical Data for Atmospheric Chemistry, Web Version, http://www.iupac-kinetic.ch.cam.ac.uk,2002.

Bailey, A. E., Heard, D. E., Paul, P. H., and Pilling, M. J.: Collisional Quenching of OH ($A^2\Sigma^+$, v'=0) by N_2, O_2 and CO_2 between 204 and 294 K. Implications for atmospheric measurements of OH by laser-induced fluorescence, J. Chem. Soc. Faraday Trans., 93, 16, 2915–2920, 1997.

Bailey, A. E., Heard, D. E., Henderson, D. A., and Paul, P. H.: Collisional quenching of OH($A^2\Sigma^+$, v'=0) by H_2O between 211 and 294 K and the development of a unified model for quenching, Chem. Phys. Lett. 302, 132–138, 1999.

Becker, K. H.: EUPHORE: Final Report to the European Commission, Contract #EV5V-CT92-0059, Bergische Universitat Wuppertal, Germany, 1996.

Becker, K. H.: In Situ Euphore Radical Measurement (EUPHORAM): Final Report to the European Commission, Contract #ENV4-CT95-0011, Bergische Universitat Wuppertal, Germany, 1999.

Bloss, W. J., Gravestock, T. J., Heard, D. E., Ingham, T., Johnson, G. P., and Lee, J. D.: Application of a compact all-solid-state laser system to the in situ detection of atmospheric OH, HO_2, NO and IO by laser-induced fluorescence, J. Environ. Monit. 5, 21–28, 2003.

Brauers, T., Aschmutat, U., Brandenburger, U., Dorn, H. P., Hausmann, M., Hessling, M., Hofzumahaus, A., Holland, F., Plass-Dülmer, C., and Ehhalt, D. H.: Intercomparison of tropospheric

OH radical measurements by multiple folded long-path laser absorption and laser-induced fluorescence, Geophys. Res. Lett. 23, 18, 2545–2548, 1996.

Cantrell, C. A., Zimmer, A., and Tyndall, G. S.: Absorption cross sections for water vapour from 183 to 193 nm, Geophys. Res. Lett. 24, 17, 2195–2198, 1997.

Calvert, J. G., Atkinson, R., Kerr, J. A., Madronich, S., Moortgat, G. K., Wallington, T. J., and Yarwood, G.: The Mechanisms of Atmospheric Oxidation of the Alkenes, OUP, New York, 2000.

Calvert, J. G., Atkinson, R., Becker, K. H., Kamens, R. M., Seinfeld, J. H., Wallington, T. J., and Yarwood, G.: The Mechanisms of Atmospheric Oxidation of Aromatic Hydrocarbons, OUP, New York, 2002.

Chan, C. Y., Hard, T. M., Mehrabzadeh, A. A., George, L. A., and O'Brien, R. A.: Third-Generation FAGE Instrument for Tropospheric Hydroxyl Radical Measurement, J. Geophys. Res. 95, D11, 18 569–18 576, 1990.

Creasey, D. J., Halford-Maw, P. A., Heard, D. E., Pilling, M. J., and Whitaker, B. J.: Implementation and initial deployment of a field instrument for the measurement of OH and HO_2 in the troposphere by laser-induced fluorescence, J. Chem. Soc., Faraday Trans., 93, 16, 2907–2913, 1997a.

Creasey, D. J., Heard, D. E., Pilling, M. J., Whitaker, B. J., Berzins, M., and Fairlie, R.: Visualisation of a supersonic free-jet expansion using laser-induced fluorescence spectroscopy: Application to the measurement of rate constants at ultralow temperatures, App. Phys. B, 65, 375–391, 1997b.

Creasey, D. J., Heard, D. E., and Lee, J. D.: Absorption cross-section measurements of water vapour and oxygen at 185 nm, Implications for the calibration of field instruments to measure OH, HO_2 and RO_2 radicals, Geophys. Res. Lett., 27, 11, 1651–1654, 2000.

Derwent, R. G., Jenkin, M. E., and Saunders, S. M.: Photochemical ozone creation potentials for a large number of reactive hydrocarbons under European conditions, Atmos. Environ., 30, 181–199, 1996.

Etzkorn, T., Klotz, B., Sørensen, S., Patroescu, I. V., Barnes, I., Becker, K. H., and Platt, U.: Gas-phase absorption cross sections of 24 monocyclic aromatic hydrocarbons in the UV and IR spectral ranges, Atmos. Environ., 33, 525–540, 1999.

Guggenheim, E. A.: On the determination of the Velocity Constant of a Unimolecular Reaction, Philos. Mag., 2, 9, 538–543, 1926.

Hard, T. M., O'Brien, R. J., Chan, Y. C., and Mehrabzadeh, A. A.: Tropospheric Free Radical Determination by FAGE, Environ. Sci. Technol., 18, 768–777, 1984.

Hard, T. M., George, L. A., and O'Brien, R. J.: An Absolute Calibration for Gas-Phase Hydroxyl Measurements, Environ. Sci. Tech., 36, 1783–1790, 2002.

Heard, D. E. and Pilling, M. J.: Measurement of OH and HO_2 in the troposphere, Chem. Rev., 103, 5163–5198, 2003.

Hofzumahaus, A., Aschmutat, U., Heßling, M., Holland, F., and Ehhalt, D. H.: The measurement of tropospheric OH radicals by laser-induced fluorescence spectroscopy during the POPCORN field campaign, Geophys. Res. Lett., 23, 18, 2541–2544, 1996.

Holland, F., Hessling, M., and Hofzumahaus, A.: In Situ Measurement of Tropospheric OH Radicals by Laser-Induced Fluorescence – A Description of the KFA Instrument, J. Atmos. Sci., 52, 19, 3393–3401, 1995.

Holland, F., Hofzumahaus, A., Schäfer, J., Kraus, A., and Pätz, H.: Measurements of OH and HO_2 radical concentrations and photolysis frequencies during BERLIOZ, J. Geophys. Res., 108, D4, 8246, doi:10.1029/2001JD001393, 2003.

Kanaya, Y., Sadanaga, Y., Hirokawa, J., Kajii, Y., and Akimoto, H.: Development of a Ground-Based LIF Instrument for Measuring HO_x Radicals: Instrumentation and Calibrations, J. Atmos. Chem., 38, 1, 73–110, 2001.

Klotz, B., Sørensen, S., Barnes, I., Becker, K. H., Etzkorn, T., Volkamer, R., and Platt, U.: Atmospheric Oxidation of Toluene in a Large-Volume Outdoor Photoreactor: In Situ Determination of Ring-Retaining Product Yields, J. Phys. Chem. A, 102, 10 289–10 299, 1998.

Lanzendorf, E. J., Hanisco, T. F., Donahue, N. M., and Wennberg, P. O.: Comment on "The measurement of tropospheric OH radicals by laser-induced fluorescence spectroscopy during the POPCORN field campaign", edited by Hofzumahaus, A. et al., and "Intercomparisons of tropospheric OH radical measurements by multiple folded long-path laser absorption and laser induced fluorescence", edited by Brauers, T. et al., Geophys. Res. Lett., 24, 23, 3037–3038, 1997.

Lee, J. D.: Development and Deployment of the FAGE instrument for measurement of HO_x in the troposphere, PhD Thesis, University of Leeds, 2000.

Levy II, H.: Normal Atmosphere: Large Radical and Formaldehyde Concentrations Predicted, Science, 173, 141–143, 1971.

Ohta, T. and Ohyama, T.: A set of rate constants for the reactions of hydroxyl radicals with aromatic hydrocarbons, Bull. Chem. Soc. Jpn., 58, 3029–3030, 1985.

Pilling, M. J.: Effects of the Oxidation of Aromatic Compounds in the Troposphere (EXACT): Final Report to the European Commission, Contract #EVK2-CT-1999-00053, University of Leeds, UK, 2003.

Perry, R. A., Atkinson, R., and Pitts Jr., J. N.: Kinetics and mechanism of the gas phase reaction of OH radicals with aromatic hydrocarbons over the temperature range 296–473 K, J. Phys. Chem., 81, 296–304, 1977.

Ravishankara, A. R., Wagner, S., Fischer, S., Smith, G., Schiff, R., Watson, R. T., Tesi, G., and Davis, D. D.: A kinetics study of the reactions of OH with several aromatic and olefinic compounds, Int. J. Chem. Kinet., 10, 783–804, 1978.

Sander, S. P., Friedl, R. R., Golden, D. M., Kurylo, M. J., Huie, R. E., Orkin, V. L., Moortgat, G. K., Ravishankara, A. R., Kolb, C. E., Molina, M. J., and Finlayson-Pitts, B. J.: Chemical Kinetics and Photochemical Data for use in Atmospheric Studies, Evaluation #14, NASA-JPL Publication 02-25, Jet Propulsion Laboratory, Pasadena, CA 91109, 2003.

Siese, M., Becker, K. H., Brockmann, K. J., Geiger, H., Hofzumahaus, A., Holland, F., Mihelcic, D., and Wirtz, K.: Direct Measurement of OH Radicals from Ozonolysis of Selected Alkenes: A EUPHORE Simulation Chamber Study, Environ. Sci. Technol., 35, 4660–4667, 2001.

Stevens, P. S., Mather, J. H., and Brune, W. H.: Measurement of tropospheric OH and HO_2 by laser-induced fluorescence at low pressure, J. Geophys. Res., 99, D2, 3543–3557, 1994.

Washida, N., Mori, Y., and Tanaka, I.: Quantum Yield of Ozone Formation from Photolysis of the Oxygen molecule at 1849 and 1931 Å, J. Chem. Phys., 54, 1119–1122, 1971.